Viser Technology Pte. Ltd.
Research and Application of Materials Science
DOI: 10.33142/rams.v3i2.6734

Research Article Open Access

Preparation and Electrochemical Performance of Si@void@NC Composite with a Tunable Nitrogen Doping Content in the Carbon Layer

Yuan QIN[1], Renzhong HUANG[2], Yan DONG[1], Liufen XIA[1], Haoran YU[1], Guodong JIANG[1*]

1 Hubei Collaborative Innovation Center for High-efficiency Utilization of Solar Energy, School of Materials and Chemical Engineering, Hubei University of Technology, Wuhan, 430068, China
2 Qingyuan Jiazhi New Materials Research Institute Co. Ltd., Qingyuan, 511517, China

***Corresponding Author:** Guodong JIANG, Hubei University of Technology, Wuhan, 430068, China, jianggd@hbut.edu.cn*

Abstract:
A strategy for the preparation nitrogen-doped carbon encapsulated Si nanocomposite with a void layer (Si@void@NC) is proposed, in which the nitrogen doping content in the carbon layer is tunable. Aniline and ortho-phenylenediamine are both selected as the nitrogen, carbon sources and co-polymerized on Si@SiO_2, in which SiO_2 is functionalized as a void template. SEM and TEM observation show that Si nanoparticles are encapsulated in a hollow and interconnected carbon cages with a thickness of less than 10 nm, which is inclined to agglomerate together to form larger particles in micrometer scale. The variation of mole ratio of aniline and ortho-phenylenediamine will enable the change of nitrogen doping level in the carbon layer and ranges from 3.2% to 8.4%. The nitrogen is doped into the carbon framework in the form of pyridinic, pyrrolic and graphitic nitrogen. Electrochemical tests indicate that the nitrogen content influences the SEI formation and the lithiation of Si nanoparticles. The potential for the decomposition of electrolyte to form SEI film and the alloying of Si-Li negatively shift when the nitrogen doping content is increased. Furthermore, the cycling performance of Si@void@NC is improved when raising the nitrogen content in the carbon. And the optimal nitrogen content is 7.5%, which is corresponding to the mole ratio of aniline to ortho-phenylenediamine is 5:5.
***Keywords:** Silicon anode; Nitrogen doping; Lithium-ion batteries*

1 Introduction

Lithium-ion batteries (LIBs) is one of the most promising energy storage devices for various applications such as portable electronics, electric vehicles, and grid scale energy storage. To satisfy the increasing demand for higher energy and power density, enormous effects have been devoted to explore advanced materials for LIBs. Among the various existing anode materials, silicon (Si), delivering the exceptional high specific capacity of 4200 $mAh{\cdot}g^{-1}$ (in the form of $Li_{4.4}Si$) is considered to be a promising alternative to commercial graphite (about 370 $mAh{\cdot}g^{-1}$) [1]. Furthermore, its other advantages, including high abundance in earth and low discharge potential (ca. 0.5 V versus Li^+/Li) also make it attractive anode materials for LIBs. Nevertheless, the commercial application of Si-based anode has been hindered by the huge volume expansion ($>300\%$), the instability of solid-electrolyte interphase (SEI) film on the Si surface and low electrical conductivity during the lithium ion insertion and extraction processes, which thus cause the degradation of the electrode and a rapid decay of the capacity. To overcome the issues, various strategies have been explored to prepare diverse structures, such as silicon nanotube, silicon nanowire, porous silicon, which enable the accommodation of the volume change [2]. Alternatively, modifying the Si nanoparticles with a carbon layer will contribute to the improvement of the performance of Si-based anode. This is because the carbon can enhance the conductivity of Si nanoparticles as well as prevent the direct contact of Si nanoparticle with the electrolyte. Particularly, it can partially alleviate the huge volume expansion [3]. Therefore, the structure and the composition of carbon will play different effects on the performance of Si nanoparticles. With regard to the further improvement of the electrical conductivity of the Si/C composites, heteroatom doping of carbon has emerged as an effective method. N, S, O and B have already been utilized as dopants to modify the electronic and crystalline structures of carbon, giving rise to the improvement of its electrochemical performance [4-8]. Among the various doping heteroatoms, nitrogen is

Received on October 22, 2021; Accepted on December 9, 2021

considered to be one of most attractive dopant in the carbon matrix, as its atomic size is comparable to that of carbon. Moreover, the high electronegativity as well as additional free electrons will contribute to the conduction band of carbon. It has been reported that the nitrogen atom incorporation increases the surface hydrophilicity of carbon-based electrodes to lithium ion, leading to the additional improvement to the capacity [9-11]. First principles calculations demonstrates that the pyridine-N and the graphite-N local structures in the carbon lattice account for the enhanced lithium storage capacity [9]. A variety of nitrogen-containing carbon sources could be chosen to achieve the nitrogen-doped carbon in Si/C composite anodes, for example, polyaniline [11-12], ethylenediamine [10] polypyrrole [13], polydopamine [14], benzenedinitrile [15], melamine [16], glucosamine[17], et al. However, using these nitrogen-containing carbon source, a certain nitrogen content in the carbon for the resulted Si/C composite is achieved. In particular, as we know, it is difficult to adjust the nitrogen content and the effect of nitrogen doping content on the electrochemical performance of Si/C composites is rarely reported.

Aniline and its derivatives are important industrial raw material used primarily for the synthesis of conducting polymer, pesticide, dye, plastic, rubber. ortho-phenylenediamine containing two amino groups will endow the derived carbon with higher nitrogen content than aniline-derived carbon. It is reported that aniline could be co-polymerized with ortho-pheneneyldiamine in a wide range mole ratio [18]. Herein, poly(ortho-phenylenediamine-co-aniline) is chosen as a nitrogen-containing carbon source for the preparation of nitrogen-doped carbon layer encapsulated silicon composites. In the composite, the nitrogen content in the carbon layer is adjustable by tuning the monomer mole ratio of aniline to ortho-phenylenediamine. The storage of lithium in the nitrogen content-tunable Si/N-doped C composites is evaluated. The results suggest a moderate level of nitrogen in the carbon layer is suitable and the prepared Si-based composites exhibit an optimal electrochemical performance.

2 Experimental Section

2.1 Materials

Nano silicon (powder, crystalline, 50-100 nm, 99%) was provide by Shanghai Chaowei Nanotechnology Co., Ltd. China. 3-aminopropyltriethoxysilane (APTES) and tetraethoxysilane (TEOS) were purchased from Shanghai Chem. Co., Ltd. Aniline (AN), ortho-phenylenediamine (oPD), ammonium peroxydisulfate (APS), and other reagents were purchased from Sinopharm Chemical Reagent Co., Ltd and were used without any purification. Deionized water was used throughout the experiments.

2.2 Synthesis of Si@void@NC composites

Simply, 0.25 g Si powder was ultrosonically dispersed into a mixture of water and alcohol (350 mL, water:alcohol (V:V)=1:4). After adding 4 mL $NH_3·H_2O$ (14.5mol/L), 0.4 mL of APTES and 3 g of TEOS were slowly dropwise added and were kept stirring for 12 h. The product was subjected to the centrigugation, washing and drying to get $Si@SiO_2$. To synthsize the copolymer-coated $Si@SiO_2$, 0.01 mol of mixed AN and oPD with a certain mole ratio was added into $Si@SiO_2$ dispersion containing 1 mol/L HCl. Then, 10 mL of 1.25 mol/L APS solution was slowly poured and the reaction was kept for 4 h. After washed and dried, $Si@SiO_2$@poly(aniline-co-ortho-phnylenediamine) composite (denoted by $Si@SiO_2$@Cp) was achieaved. Afterward, $Si@SiO_2$@Cp composite was subjected to the carbonization at 800 °C for 2 h in an Ar atomsphere with a ramping rate of 2 °C/min, then $Si@SiO_2$@nitrogen-doped carbon ($Si@SiO_2$@NC) composite was obtained. Finally, SiO_2 was ethced by 5 %(wt) HF solution to get Si@void@nitrogen-doped C composites, which was assigned to Si@void@NC. The nitrogen doping content in the carbon of Si@void@NC was tuned by changing the mole ratio of AN to oPD from 10:0, 8:2, 5:5 to 2:8, which were assigned to Si@void@NC-1, Si@void@NC-2, Si@void@NC-3 and Si@void@NC-4, respetively.

2.3 Characterizations

X-ray photoelectron spectroscopy (XPS) spectra were taken on VG Multilab 2000 photoelectron spectrometer. Attenuated total reflection Fourier transform infrared (FT-IR) spectra were collected on Thermo Scientific Nicolet iS 50 with the wavenumber of 4000-600 cm^{-1}. The phase structures were analyzed and identified by X-ray diffractometer (Empyrean B.V. Holland) with a Cu K_α radiation. The morphology and structure were observed on field emission scanning electron microscopy (Hitachi SU8010) and transmission electron microscopy (JOEL 2100F), respectively.

2.4 Cells assemble and electrochemical measurements

A homogeneous slurry consisting of active material, carbon black (Super P) and sodium carboxymethyl cellulose (CMC) with a weight ratio of 8:1:1 to was coated on Cu foil by doctor-blade method. After drying at 60°C in vacuum overnight, the Cu foil was punched into 12 mm diameter discs with an effective mass loading of 0.5-0.7 mg/cm^2. Then the two-electrode coin-type cells (CR2032) were assembled in an Ar-filled glovebox with Li metal foil as counter and reference electrode, 1 M $LiPF_6$ dissolved in the mixture of ethylene carbonate (EC), dimethyl carbonate (DMC) and diethyl carbonate (DEC) (1:1:1 in volume) as the electrolyte and Celgard 2300 membrane as the separator. The galvanostatic charge/discharge tests were carried out on Land CT2001A battery test system in a potential range of 0.01-1.5 V (vs. Li/Li^+). The capacity is calculated based on the mass of

Si@void@NC composite on the electrode. The cyclic voltammetry (CV) and electrochemical impedance spectroscopy (EIS) measurements were conducted on Zahner Zennium (Germany) electrochemical workstation. All the electrochemical measurements were conducted at room temperature.

3 Results and Discussion

The preparation procedure of Si@void@NC composites is schematically illustrated in Figure 1. Firstly, Si nanoparticles is modified by a SiO_2 coating through the hydrolysis of APTES and TEOS, which functions as a void templet between the carbon layer and Si nanoparticles. The addition of APTES favors the uniform cover of the copolymer due to the amino group. After the co-polymerization of AN and o-PD on SiO_2 coating and the carbonization at an inert atmosphere, SiO_2 coating is etched by HF solution. The molar ratio of AN to o-PD is changed to adjust the doping level of nitrogen atoms in the final Si@void@NC composites.

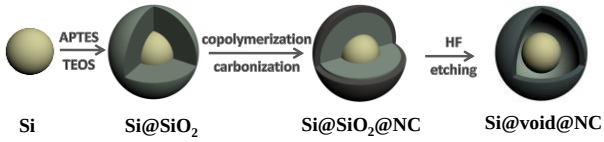

Figure 1 Schematic illustration of the preparation processes of Si@void@NC composites

The molecular structure of different samples is inverstigated to observe the evolution of Si nanoparticles by FT-IR spectroscopy. Figure 2(a). displays FT-IR spectra of samples acquired at the different steps during the preparation of Si@void@NC composites. The pristine Si nanopaticles show several adsorption peaks due to Si-O-Si stretching (1170 cm^{-1} and 1080 cm^{-1}) and bending vibrations (883 cm^{-1} and 830 cm^{-1}) [19]. Contrast to pristine Si nanoparticles, Si@SiO_2@Cp shows several strong absorption bands between 1700 cm^{-1} and 900 cm^{-1}. The peaks at 1537 cm^{-1} and 1486 cm^{-1} are the stretching vabration of the qiunoid and benzenoid rings in polyaniline [20], respectively. The band at 1631 cm^{-1} suggests the existence of oPD in the copolymer [21]. Most importantly, the occurrence of the bands at 1370 cm^{-1}, 1060 cm^{-1} and 892 cm^{-1} proves the phenzaine-like cyclic structure in the copolymer backbone [21-22], which could either be attributed to the presence of poly(ortho-phenylenediamine) blocks or the cyclic formation of the adjacent oPD and AN unit in the copolymeric chain, comfiring the copolymerization of AN and oPD. After the carbonization of Si@SiO_2@Cp in an inert atmosphere, the copolymer will be converted to the nitrogen doped carbon materials. Meamwhile, the typical absorption bands of the copolymer will vanish. It is found that the structure of the composite isn't damaged by HF acid etching besides the removal of SiO_2.

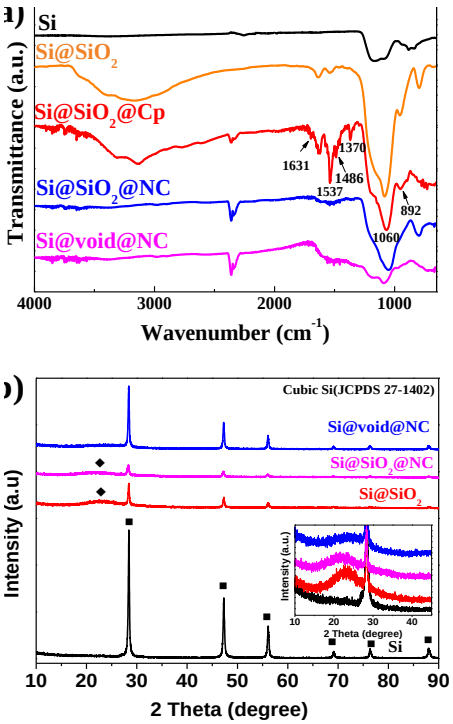

Figure 2 (a) FT-IR spectra and (b) XRD patterns of different samples. The inset in Figure b is the magnification in range of 10 to 45 degree. (■—Si, ◆—SiO_2)

The crystalline structure of different Si-based samples is futher investigated by X-ray diffraction spectroscopy (XRD), as shown in Figure 2(b). The pristine Si nanoparticles are crystalline and show several sharp diffraction peaks at 28.5 °,47.3 °, 56.1 °, 69.0 °, 76.3 ° and 88.0 °, which can be indexed to (111), (220), (311), (400), (331) and (422) lattice planes of cubic Si (JCPDS NO. 27-1402), respectively. Once SiO_2 is deposited on the surface of Si nanoparticles, a broad and weak band centred at 23° is observed, which is due to the diffraction of amorphous SiO_2. While the copolymer of AN and oPD is formed and further converted to the nitrogen-doped carbon layer on SiO_2, there is no new peak observed in the diffraction pattern and the diffraction profile almost does not change besides the further decline in the diffraction strenghth. At the same time, the weak and broad peak near 23° still exsits. However, once treated by the HF etching, the diffraction corresponding SiO_2 is weakened and shifted to a higher angle. Additionally, the peak strenghth for Si nanoparticles drastically increases, implying SiO_2 layer is removed and the space between Si and nitrogen-doped carbon is created.

SEM images of pristine Si nanopartilces (Figure 3(a,b)) show that they are predominantly spherical in the shape with a diameter ranging from 50 nm to 100 nm. The modification of Si nanoparticles by SiO_2 results in a slight increase in the size. Meanwhile, some Si@SiO_2 particles aggregate together, as shown in Figure 3(c,d). In contrast, the remarkable change in the morphology and size for the Si@void@NC is observed in Figure 3(e,f).

The agglomeration of Si@SiO_2@Cp during the surface polymerizaton and carbonization may acccount for the structure change for Si@void@NC.

The internal structure of Si@void@NC is investigated by TEM, as displayed in Figure 3(g, h). The agglomerated Si@void@NC is evident, which is in accordance with the results of SEM. It is noted that Si nanoparticles are successfully encapsulated inside the interconnected nitrogen-doped carbon cage.It is seen that the nitrogen-doped carbon cage is very thin and has a thickness of less than 10 nm. Additionally, a void between Si nanoparticle and the thin carbon layer is generated. The void place presented in Si-based composite nanoparticle will accommodate the expansion during the lithiation of Si and stabilize the electrode.

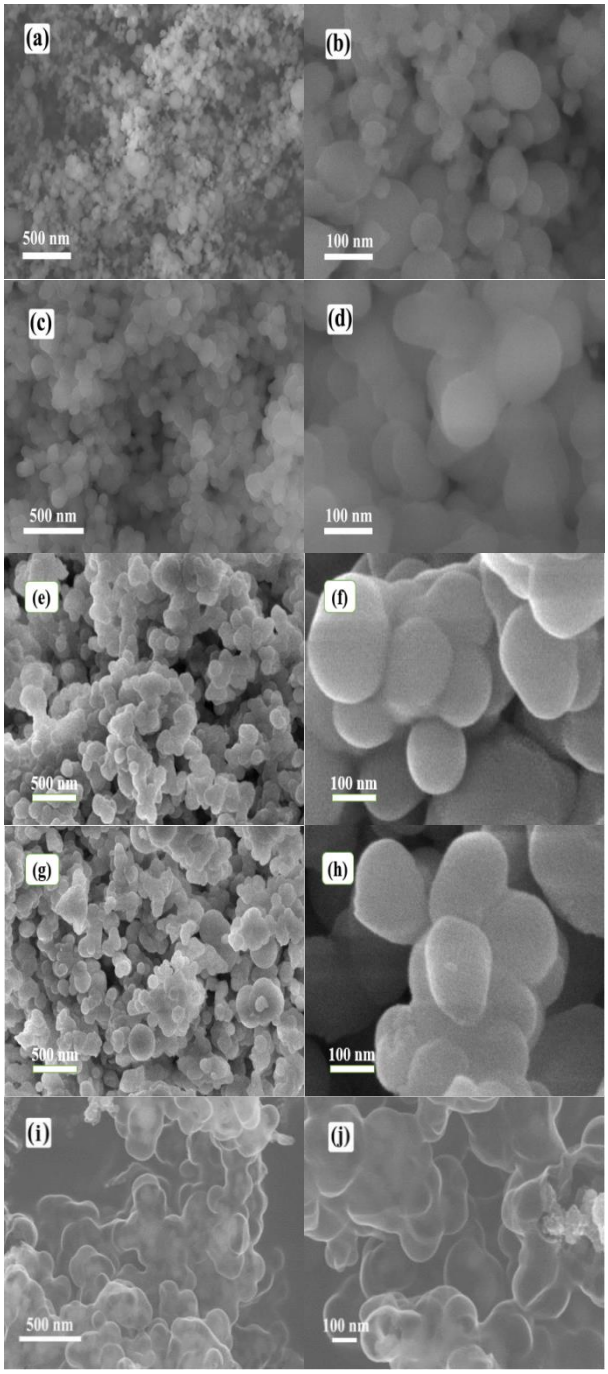

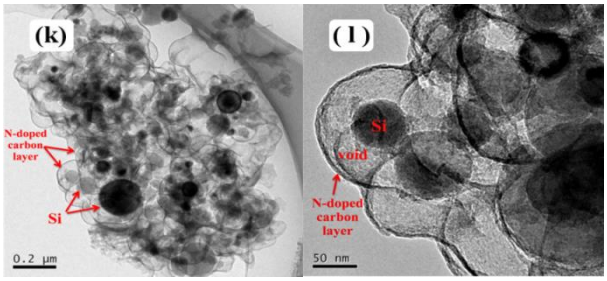

Figure 3 SEM (a-j) and TEM (k-l) images of (a, b) pristine Si, (c,d) Si@SiO_2 ,(e,f) Si@SiO_2@Cp , (g,h) Si@SiO_2@NC and (i-l) Si@void@NC

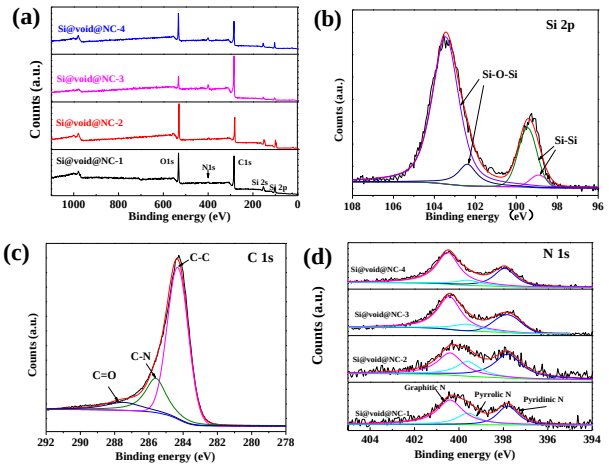

Figure 4 (a) XPS survey spectra of Si@void@NC samples and the high-resolution spectra of (b) Si 2p, (c) C 1s in Si@void@NC-3 and (d) N 1s in different Si@void@NC samples

Table 1 The relative nitrogen contents of Si@void@C in different ratio of An to OPD

Sample	Si@void@N C-1	Si@void@NC-2	Si@void@NC-3	Si@void@NC-4
Nitrogen content (vs. carbon)	3.2%	4.0%	7.5%	8.4%

Figure 4(a) shows the X-ray photoelectron spectroscopy (XPS) survey spectra of Si@void@NC samples. It is confirmed that both the carbon and nitrogen elements exist in all Si@void@NC samples, implying the nitrogen is doped into the carbon lattice. Moreover, the increase in the relative peak strength of nitrogen to carbon with the increase of the mole ratio of o-PD to AN suggests that the nitrogen level in the carbon layer gradually raises. According to the peak area of nitrogen and carbon, the relative atomic content of nitrogen in the carbon layer is calculated and the results are shown in Table 1. The nitrogen content of 3.2% is achieved while only AN is polymerized on Si@SiO_2. However, once AN is copolymerized with oPD, the nitrogen content is increased and the content is 4.0%, 7.5% and 8.4% for Si@void@NC-2, Si@void@NC-3, Si@void@NC-4,

respectively. Accordingly, the nitrogen doping content in the carbon layer is readily tuned by the copolymerization of AN and o-PD. The chemical state of Si, C and N is studied by their corresponding fine XPS spectra. Figure 4(b) shows the Si 2p spectrum. The peaks with the binding energy of 98.9 eV and 99.5 eV are assigned to Si-Si bond, while the peaks centering at 102.3 eV and 103.1 eV are attributed to SiO_x owing to the sight oxidation of Si nanoparticles [13-23]. The C1s peak in Figure 4(c) consists of three sub-peaks located at 284.4 eV, 285.7 eV and 287.7 eV corresponding to C-C C-N and C=O, respectively. The existence of N-C bond is due to the substitution of N atoms, suggesting the successful N-doping into the carbon framework [10-17]. The N 1s high-resolution XPS spectrum can be deconvoluted into three peaks located at 397.8 eV, 399.7 eV and 400.4 eV, respectively, which are associated with the pyridinic, pyrrolic and graphitic nitrogen atoms doped into the carbon framework [12-17]. The nitrogen doping in the carbon layer is beneficial to achieve high electronic conductivity and provides additional lithium storage sites, boosting the performance of Si anode. Moreover, more oPD seems to cause a high content of graphitic and pyridinic nitrogen, which facilitates the lithium intercalation [9].

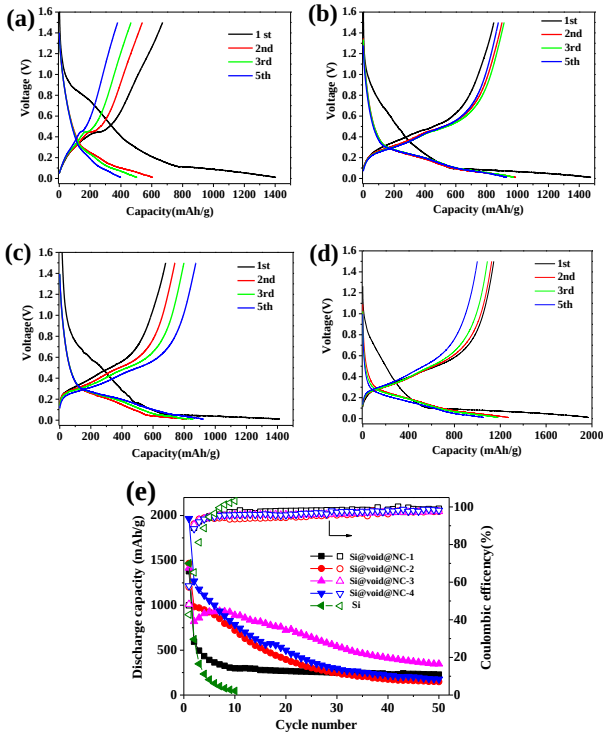

Figure 5 (a-d) The charge-discharge curves of the 1st-3rd, 5th cycles for (a) Si@void@NC-1, (b) Si@void@NC-2, (c) Si@void@NC-3 and (d) Si@void@NC-4 and (e) cycling perfance and coulombic efficency of Si and Si@void@NC at current density of 100 mA/g at a current density of 100 mA/g

The charge and discharge profiles of the four Si@void@NC samples for the 1st, 2nd, 3rd, 5th cycle at a current density of 100 mA/g are displayed in Figure 5. For all the samples, the similarity of their profiles in the first charge/discharge cycle demonstrates that the electrochemical reaction of lithium in these Si@void@NC composites has no distinct difference. A long slope plateau in the charge process from 1.0 to 0.20 V will vanish in the subsequent cycles, resulting in the irreversible consumption of lithium and the formation of the SEI film. The slope profile between 0.1 V and 0.01 V is considered to be the lithiation of Si. All the Si@void@NC samples deliver an initial discharge capacity of over 1400 mAh/g in the first cycle. The discharge capacity gradually decrease during the charge-discharge cycle. When the mole ratio of AN to o-PD is fixed at 5:5, the capacity fading is the slowest. It is noteworthy that a charge plateau is present near 0.4 V for Si@void@NC especially noticeable for the sample Si@void@NC. This is ascribed to the dealloying process of Si nanoparticles [24].

The cycling performance of Si@void@NC has been evaluated using galvanostatic charge-discharge measurements at a current density of 100 mA/g with the lower and upper cutoff voltages of 0.01 V and 1.5 V (Figure 5(e)). Si@void@NC-1 prepared only using polyaniline as carbon and nitrogen sources delivers an initial capacity of 1378 mAh/g, but rapidly reduces to 594 mAh/g for the second cycle. Subsequently, the discharge capacity decays and a low capacity of 227 mAh/g is remained at 50th cycle. However, with the increase of the concentration of o-PD during the polymerization, implying the increase of nitrogen doping content in the carbon layer, the capacity decay becomes slow. It is evident that Si@void@NC-3 manifests the best cycle stability and a capacity of 346 mAh/g is retained, suggesting too high nitrogen content in the carbon layer may deteriorate the performance of Si@void@NC. Besides, the coulombic efficiency of the four samples for the first cycle is about 47%-58%, and quickly reaches above 95%. Nevertheless, the results are not satisfactory in terms of the cycling stability. This may be due to the structure of Si@void@NC, which is needed to optimize further such as the void volume, the thickness of carbon layer.

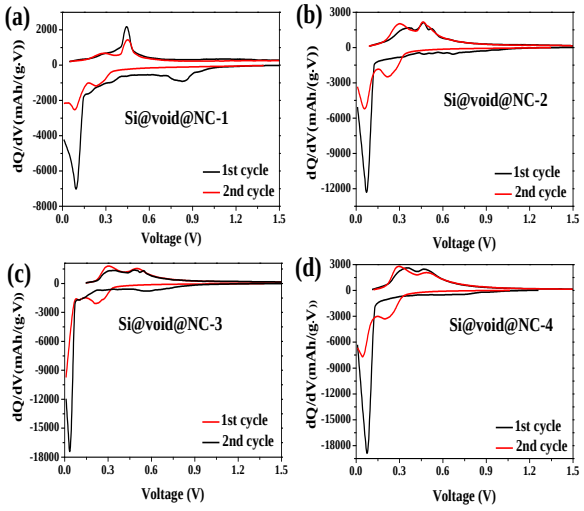

Figure 6 The differential capacity curves of (a) Si@void@NC-1, (b) Si@void@NC-2, (c) Si@void@NC-3 and (d) Si@void@NC-4

The electrochemical lithiation and delithiantion reaction of Si nanoparticles is able to be observed detailly in the differantial capacity curves (dQ/dV) [25]. Figure 6 displays the differential capacity curves of Si@void@NC samples for the first two cycle. During the discharge process, all the samples encounter the SEI formation (between 0.4V and 1.0V) and the lithiation (below 0.1 V). It is notewrothy that SEI formation and lithiation of Si nanoparticle require a lower potential, verified by left shift of the peaks corresponding to SEI formation and lithiation, when oPD is added. This is mightly caused by the increase of nitrogen content in the carbon layer. It is reported that Pyridinic and pyrrolic N species are more active because they can induce defects and edge sites in carbon material, favoring the diffusion and insert into the carbon [26]. In the research, higher oPD will introduce more nitrogen atom in the carbon layer. And there are three type of nitrogen species in the carbon layer, namely pyrrolic N and pyridinic N and graphitc N. As seen in figure 4(e), when nitrogen content in the carbon is increased, the ratio of graphtic N to pyrrolic N and pyridinic N raises. Therefore, low pyridinic and pyrrolic N will reduce the reaction actively of lithium ion, then a lower potential is required for the formation of SEI film. During the discharge, two peaks corresponding to the delithiation of Si-Li alloy are persent. In the second cycle, besides the reaction potential, there is not significatanly difference in the lithiaion and delithiation of amorphous Si converted in the first cycle, demonstating that the nitrogen doping level will affect the lithiantion and delithiation difficulty of Si nanoparticle. In terms of capacity fading during the cycle, the mole ratio of 5:5 for AN to o-PD is optimal.

4 Conclusion

A Si@void@NC nanocomposite with a tunable nitrogen content in the carbon layer is prepared. In the composite, a void between Si core and carbon layer is created through the etching of SiO_2 template. And AN and oPD is co-polymerized and utilized as nitrogen-containing carbon source, in which the mole ratio of AN and oPD can is varied to modulate the nitrogen doping level in the carbon layer. The characterization shows that Si@void@NC is inclined to agglomerate together to form larger particles in micrometer scale the copolymerization and carbonization, in which Si nanoparticles are encapsulated in a hollow and interconnected carbon cages with a thickness of less than 10 nm. It is found that the nitrogen content in the carbon layer varies from 3.2% to 8.4%. Moreover, the nitrogen doping into the carbon are present in the form of pyridinic, pyrrolic and graphitic nitrogen, regardless of its content in the carbon. Electrochemical tests indicate that the SEI formation and the lithiation of Si nanoparticles become difficult as the nitrogen doping content is raised. Additionally, the capacity fading is inhibited for Si@void@NC with a suitable nitrogen content. Compared to a capacity of 227 mAh/g for Si@void@NC-1 derived only from polyaniline, a capacity of 346 mAh/g is remained after 50 charge-discharge cycles for Si@void@NC-3 prepared with the mole ratio of 5:5 for AN and oPD. Nonetheless, the cycling stability is not satisfactory, which may be improved by the optimization of the preparation conditions and the structure of Si@void@NC.

Author Contributions: Y. Qin conducted the preparation and properties of the materials and wrote this manuscript; R. Huang and Y. Dong performed the characterization of the materials; L. Xia performed the data analysis; H. Yu contributed significantly to manuscript preparation; G. Jiang helped perform the analysis with constructive discussions and will be responsible for this article.

Conflict of Interest: The authors declare that there is no conflict of interest regarding the publication of this paper.

Acknowledgments: This work was supported by grants Hubei Province Technology Innovation Project (2018AAA056), Open Fund of Hubei Collaborative Innovation Center for High Efficient Utilization of Solar Energy (HBSKFZD2017006) and Innovative Research and Development Institute of Guangdong (No. 2018B090902009), Innovation and entrepreneurship training program for College Students (No.201710500024).

References

[1] Su X, Wu Q, Li J, et al. Silicon-based nanomaterials for lithium-ion batteries: a review. Adv Energy Mater 2014, 4: 1300882.

[2] Rahman M A, Song G, Bhatt A I, et al. Nanostructured silicon anodes for high-performance lithium-ion batteries. Adv Funct Mater 2016, 26: 647-678.

[3] Fang G, Deng X, Zou J, et al. Amorphous/ordered dual carbon coated silicon nanoparticles as anode to enhance cycle performance in lithium ion batteries. Electrochim Acta 2019, 295: 498-506.

[4] Chen L F, Huang Z H, Liang H W, et al. Three-dimensional heteroatom-doped carbon nanofiber networks derived from bacterial cellulose for supercapacitors. Adv Funct Mater 2014, 24: 5104-5111.

[5] Li Y J, Wang G L, Wei T, et al. Nitrogen and sulfur co-doped porous carbon nanosheets derived from willow catkin for supercapacitors. Nano Energy 2016, 19: 165-175.

[6] Qie L, Chen W M, Xiong X Q, et al. Sulfur-doped carbon with enlarged interlayer distance as a high-performance anode material for sodium-ion batteries. Advanced Science 2015, 2: 1500195.

[7] Liu X H, Zhang L Q, Zhong L, et al. Ultrafast ele° trochemical lithiation of individual si nanowire anodes. Nano Lett 2011, 11: 2251-2258.

[8] Paraknowitsch J P, Thomas A. Doping carbons beyond nitrogen: an overview of advanced heteroatom doped carbons with boron, sulphur and phosphorus for energy

applications. Energ Environ Sci 2013, 6: 2839-2855.
[9] Cho Y J, Kim H S, Im H, et al. Nitrogen-doped graphitic layers deposited on silicon nanowires for efficient lithium-ion battery anodes. J Phys Chem C 2011, 115: 9451-9457.
[10] Jeong M G, Islam M, Du H L, et al. Nitrogen-doped carbon coated porous silicon as high performance anode material for lithium-ion batteries. Electrochim Acta 2016, 209: 299-307.
[11] Tao H C, Huang M, Fan L Z, et al. Effect of nitrogen on the electrochemical performance of core–shell structured Si/C nanocomposites as anode materials for Li-ion batteries. Electrochim Acta 2013, 89: 394-399.
[12] Xu R, Wang G, Zhou T, et al. Rational design of Si@carbon with robust hierarchically porous custard-apple-like structure to boost lithium storage. Nano Energy 2017, 39: 253-261.
[13] Lu B, Ma B, Deng X, et al. Cornlike Ordered mesoporous silicon particles modified by nitrogen-doped carbon layer for the application of li-ion battery. ACS Appl Mater Interfaces 2017, 9: 32829-32839.
[14] Jung C H, Choi J, Kim W S, et al. A nanopore-embedded graphitic carbon shell on silicon anode for high performance lithium ion batteries. J Mate. Chem C 2018, 6: 8013-8020.
[15] Zhu J, Yang J, Xu Z, et al. Silicon anodes protected by a nitrogen-doped porous carbon shell for high-performance lithium-ion batteries. Nanoscale 2017, 9: 8871-8878.
[16] Mu T, Zuo P, Lou S, et al. A two-dimensional nitrogen-rich carbon/silicon composite as high performance anode material for lithium ion batteries. Chem Eng J 2018, 341: 37-46.
[17] Ji D, Wan Y, Yang Z, et al. Nitrogen-doped graphene enwrapped silicon nanoparticles with nitrogen-doped carbon shell: a novel nanocomposite for lithium-ion batteries. Electrochim Acta 2016, 192: 22-29.
[18] Roković M K, Jurišić A, Žic M, et al. Manipulation of polymer layer characteristics by electrochemical polymerization from mixtures of aniline and ortho-phenylenediamine monomers. J Appl Polym Sci 2009, 113: 427-436.
[19] Zhang L, Liu Y, Key B, et al. Silicon Nanoparticles: Stability in Aqueous Slurries and the Optimization of the Oxide Layer Thickness for Optimal Electrochemical Performance. ACS Appl Mater Interfaces 2017, 9: 32727-32736.
[20] Olmedo-Martínez J L, Farías-Mancilla B I, Vega-Rios A, et al. Poly(ortho-phenylenediamine-co-aniline) based copolymer with improved capacitance. J Power Sources 2017, 366: 233-240.
[21] Parsa A., Ab Ghani S. Electrocopolymerization of aniline and ortho-phenylenediamine via facile negative shift of polyaniline redox peaks. Polymer 2008, 49, 3702-3708.
[22] Zhang L, Yuan W, Yan Y. In situ UV–vis spectroeletrochemical studies on the copolymerization of o-phenylenediamine and o-methoxy aniline. Electrochim Acta 2013, 113: 218-228.
[23] Zhang Y C, You Y, Xin S, et al. Rice husk-derived hierarchical silicon/nitrogen-doped carbon/carbon nanotube spheres as low-cost and high-capacity anodes for lithium-ion batteries. Nano Energy 2016, 25: 120-127.
[24] Lin N, Zhou J, Wang L, et al. Polyaniline-assisted synthesis of Si@C/RGO as anode material for rechargeable lithium-ion batteries. ACS Appl Mater Interfaces 2015, 7: 409-414.
[25] Obrovac M N, Krause L J. Reversible cycling of crystalline silicon powder. J Electrochem Soc 2007, 154: A103-A108.
[26] Luan Y, Hu R, Fang Y, et al. Nitrogen and phosphorus dual-doped multilayer graphene as universal anode for full carbon-based lithium and potassium ion capacitors. Nano-Micro Letters, 2019, 11 (1): 30-31.